THREE-DIMENSIONAL MULTIPHASE BLACK-OIL SIMULATOR BASED ON GLOBAL MASS FRACTION

Wilgo Moreira Nunes, iugoslavo@gmail.com[a]
Duarte da Costa Sarmento, duartecosta_sarmento@yahoo.co.id[b]
Federal University of Ceará – Mechanical Engineering Department[a], Chemical Engineering Department[b]

André Luiz de Souza Araújo, andre@ifce.edu.br
Instituto Federal de Educação, Ciência e Tecnologia do Ceará

Francisco Marcondes, marcondes@ufc.br
Federal University of Ceará – Department of Metallurgical Engineering and Material Science

Abstract. *In general, petroleum reservoir simulators for the black-oil model are based on pressure and saturation. However, to deal with the gas phase appearance/disappearance some numerical tricks are necessary. In order to avoid this problem, this paper presents the black-oil model in terms of pressure and mass molar fraction. The equations are discretized through the finite-volume method using boundary-fitted coordinates. The results are presented in terms of volumetric rates and saturation for oil, gas, and water phases. Also, the results are compared with the commercial simulator IMEX from CMG company.*

Keywords*: Multiphase flow, Global mass fraction, Boundary-fitted coordinates, Finite-volume method*

1. INTRODUCTION

The unknowns in most of petroleum reservoir simulators, based on black-oil model, are pressure and saturations. However, to deal with the gas phase appearance/disappearance some numerical procedures are necessary. These procedures include, for instance, some gas residual saturation or change the variables during the simulation when the gas phase appear or disappear, Maliska et al. (1997). On alternative approach to by-pass this numerical problem is to replace the phase saturation by the global mass fraction as suggested by Prais and Campagnolo (1981). In this approach, even when all gas phase is dissolved in oil phase the global mass fraction of gas will be different from zero, Maliska et al. (1997).

In this paper the above mentioned approach is applied to multiphase flows involving oil, gas, and water in conjunction with boundary-fitted coordinates. The mass balance equations in terms of global mass fraction of oil, gas and water are discretized through the finite-volume method and linearized by the Newton's method. The results are presented in terms of volumetric rates of oil, gas, and water and phase saturations.

2. PHYSICAL MODEL

The black-oil equations for the water, oil, and gas components in terms of the global mass fractions and pressures are given by

$$\frac{\partial}{\partial t}\left(\phi \rho_m Z_w\right) = \nabla.\left(\lambda_w \bar{\bar{K}}.\nabla \Phi_w\right) - \bar{m}_w \tag{1}$$

$$\frac{\partial}{\partial t}\left(\phi \rho_m Z_o\right) = \nabla.\left(X_{oo}\lambda_o \bar{\bar{K}}.\nabla \Phi_o\right) - X_{oo}\bar{m}_o \tag{2}$$

$$\frac{\partial}{\partial t}\left(\phi \rho_m Z_g\right) = \nabla.\left(\left(1-X_{oo}\right)\lambda_o \bar{\bar{K}}.\nabla \Phi_o + \lambda_g \bar{\bar{K}}.\nabla \Phi_g\right) - \left(1-X_{oo}\right)\bar{m}_o - \bar{m}_g \tag{3}$$

Summing Equations (1) thorough (3) the following global mass conservation equation is obtained:

$$\frac{\partial}{\partial t}\left(\phi \rho_m\right) = \nabla.\left(\lambda_w \bar{\bar{K}}.\nabla \Phi_w + \lambda_o \bar{\bar{K}}.\nabla \Phi_o + \lambda_g \bar{\bar{K}}.\nabla \Phi_g\right) - \bar{m}_w - \bar{m}_o - \bar{m}_g \tag{4}$$

Equation (4), in this work, will be called pressure equation. In Eqs. (1) through (4), ϕ denote the porosity, ρ_m the average density, Z_w, Z_o, Z_g are respectively the water, oil, and gas global mass fractions, X_{oo} the mass fraction of

component oil in oil phase, λ_w, λ_o, λ_g are respectively, the water, oil, and gas phases multiplied by the density of the each phase, $\bar{m}_w, \bar{m}_o, \bar{m}_g$ are the mass flow rate of water, oil and gas phases, respectively per unit of bulk volume of the reservoir. These terms represent the sink or source terms for the control volumes which could contain a well. $\bar{\bar{K}}$ is the absolute permeability tensor which is assumed, in this work, as a diagonal tensor. The potential of each phase (Φ) is given by

$$\Phi_p = P_p - \rho_p\, g\, z \tag{5}$$

where p denotes the water, oil, or gas phase, P is the pressure, ρ_p is the density of phase p, g is gravity, and z is the depth, which is positive in the upward direction. Inspecting Eqs. (1) through (5), we can seen that there are 6 unknowns for (Z_w, Z_o, Z_g, P_w, P_o, and P_g) and only three equations, since Eq. (4) is just a combination of Eqs. (1) through (3). The closing equations comes from capillarity pressure relations and the mass conservation equation which requires

$$Z_w + Z_o + Z_g = 1 \tag{6}$$

3. EVALUATION OF THE PHYSICAL PROPERTIES

In order to evaluate the physical properties a flash calculation procedure as suggested by Prais and Campagnolo (1981) and Cunha (1996) will be used. In this procedure, we first evaluate the gas-oil solubility ratio by

$$R_s = \min\left\{ \frac{\rho_{o,STC}}{\rho_{SgTC}} \frac{(1 - Z_o - Z_w)}{Z_o}, R_s(P_o) \right\} \tag{7}$$

where STC means standard conditions and Rs(P_o) denotes the gas-oil solubility ratio in PVT data of Black-oil model. Then, we evaluate the mass fraction of each phase (α_p). The mass fraction of water, oil, and gas phase are given by

$$\alpha_w = Z_w \;\; ; \;\; \alpha_o = Z_o\left[1 + \frac{\rho_{o,STC}}{\rho_{SgTC}} R_s \right] \;\; ; \;\; \alpha_g = 1 - \alpha_w - \alpha_o \tag{8}$$

Further details of the mass fraction of each phase can be found in Cunha (1996). The next step is to evaluate the density of each phase, and finally the saturations. The saturations are evaluated by

$$\alpha_p = \frac{\dfrac{\alpha_p}{\rho_p}}{\sum\limits_{np} \dfrac{\alpha_p}{\rho_p}} \tag{9}$$

where n_p denotes the number of phases.

4. TRANSFORMATION OF THE EQUATIONS

In this work Eqs. (1), (2), and (4) are used to evaluate Z_w, Z_o, and P_o. In order to deal with complex features of the reservoirs such as irregular boundaries and faults, boundary-fitted coordinates are employed. The equations are written in computational plane using the following transformation:

$$\xi = \xi(x, y, z) \;\; ; \;\; \eta = \eta(x, y, z) \;\; ; \;\; \gamma = \gamma(x, y, z) \tag{10}$$

Using the relations given by Eq. (10), Eqs. (1), (2), (4) can be written in a regular computational plane, Thompson et al. (1985) and Maliska (2004). Therefore, the following equations for the components water, oil and the pressure equations are obtained in the computational plane:

Water equation:

$$\frac{\partial}{\partial t}\left(\frac{\phi \rho_m Z_w}{J_t}\right) = \frac{\partial}{\partial \xi}\left[D_{11w}\frac{\partial \Phi_w}{\partial \xi} + D_{12w}\frac{\partial \Phi_w}{\partial \eta} + D_{13w}\frac{\partial \Phi_w}{\partial \gamma}\right] + \frac{\partial}{\partial \eta}\left[D_{21w}\frac{\partial \Phi_w}{\partial \xi} + D_{22w}\frac{\partial \Phi_w}{\partial \eta} + D_{23w}\frac{\partial \Phi_w}{\partial \gamma}\right] +$$

$$\frac{\partial}{\partial \gamma}\left[D_{31w}\frac{\partial \Phi_w}{\partial \xi} + D_{32w}\frac{\partial \Phi_w}{\partial \eta} + D_{33w}\frac{\partial \Phi_w}{\partial \gamma}\right] - \frac{\overline{m}_w}{J_t} \tag{11}$$

Oil equation:

$$\frac{\partial}{\partial t}\left(\frac{\phi \rho_m Z_o}{J_t}\right) = \frac{\partial}{\partial \xi}\left[X_{oo}\left(D_{11o}\frac{\partial \Phi_o}{\partial \xi} + D_{12o}\frac{\partial \Phi_o}{\partial \eta} + D_{13o}\frac{\partial \Phi_o}{\partial \gamma}\right)\right] + \frac{\partial}{\partial \eta}\left[X_{oo}\left(D_{21o}\frac{\partial \Phi_o}{\partial \xi} + D_{22o}\frac{\partial \Phi_o}{\partial \eta}\right.\right.$$

$$+\frac{\partial}{\partial \gamma}\left[X_{oo}\left(D_{31o}\frac{\partial \Phi_o}{\partial \xi} + D_{32o}\frac{\partial \Phi_o}{\partial \eta} + D_{33w}\frac{\partial \Phi_o}{\partial \gamma}\right)\right] - \frac{\overline{m}_o}{J_t} \tag{12}$$

Pressure equation:

$$\frac{\partial}{\partial t}\left(\frac{\phi \rho_m}{J_t}\right) = \frac{\partial}{\partial \xi}\left[D_{11w}\frac{\partial \Phi_w}{\partial \xi} + D_{12w}\frac{\partial \Phi_w}{\partial \eta} + D_{13w}\frac{\partial \Phi_w}{\partial \gamma}\right] + \frac{\partial}{\partial \eta}\left[D_{21w}\frac{\partial \Phi_w}{\partial \xi} + D_{22w}\frac{\partial \Phi_w}{\partial \eta} + D_{23w}\frac{\partial \Phi_w}{\partial \gamma}\right] +$$

$$\frac{\partial}{\partial \gamma}\left[D_{31w}\frac{\partial \Phi_w}{\partial \xi} + D_{32w}\frac{\partial \Phi_w}{\partial \eta} + D_{33w}\frac{\partial \Phi_w}{\partial \gamma}\right] + \frac{\partial}{\partial \xi}\left[\left(D_{11o}\frac{\partial \Phi_o}{\partial \xi} + D_{12o}\frac{\partial \Phi_o}{\partial \eta} + D_{13o}\frac{\partial \Phi_o}{\partial \gamma}\right)\right] +$$

$$\frac{\partial}{\partial \eta}\left[\left(D_{21o}\frac{\partial \Phi_o}{\partial \xi} + D_{22o}\frac{\partial \Phi_o}{\partial \eta} + D_{23o}\frac{\partial \Phi_o}{\partial \gamma}\right)\right] + \frac{\partial}{\partial \gamma}\left[\left(D_{31o}\frac{\partial \Phi_o}{\partial \xi} + D_{32o}\frac{\partial \Phi_o}{\partial \eta} + D_{33o}\frac{\partial \Phi_o}{\partial \gamma}\right)\right] + \tag{13}$$

$$\frac{\partial}{\partial \xi}\left[D_{11g}\frac{\partial \Phi_g}{\partial \xi} + D_{12g}\frac{\partial \Phi_g}{\partial \eta} + D_{13g}\frac{\partial \Phi_g}{\partial \gamma}\right] + \frac{\partial}{\partial \eta}\left[D_{21g}\frac{\partial \Phi_g}{\partial \xi} + D_{22g}\frac{\partial \Phi_g}{\partial \eta} + D_{23g}\frac{\partial \Phi_g}{\partial \gamma}\right] +$$

$$\frac{\partial}{\partial \gamma}\left[D_{31g}\frac{\partial \Phi_g}{\partial \xi} + D_{32g}\frac{\partial \Phi_g}{\partial \eta} + D_{33g}\frac{\partial \Phi_g}{\partial \gamma}\right] - \frac{\overline{m}_w + \overline{m}_o + \overline{m}_g}{J_t}$$

In the transformed equations J_t is the Jacobian of the transformation and D tensor involves fluid, reservoir and geometric information. The expression for the Jacobian and D tensor for the water component are given by

$$D_{11w} = \frac{\lambda_w}{J_t}\left(\xi_x^2 K_{xx} + \xi_y^2 K_{yy} + \xi_z^2 K_{zz}\right) \; ; \; D_{12w} = \frac{\lambda_w}{J_t}\left(\xi_x \eta_x K_{xx} + \xi_y \eta_y K_{yy} + \xi_z \eta_z K_{zz}\right) = D_{21w}$$

$$D_{13w} = \frac{\lambda_w}{J_t}\left(\xi_x \gamma_x K_{xx} + \xi_y \gamma_y K_{yy} + \xi_z \gamma_z K_{zz}\right) = D_{31w} \; ; \; D_{22w} = \frac{\lambda_w}{J_t}\left(\eta_x^2 K_{xx} + \eta_y^2 K_{yy} + \eta_z^2 K_{zz}\right) \tag{14}$$

$$D_{23w} = \frac{\lambda_w}{J_t}\left(\eta_x \gamma_x K_{xx} + \eta_y \gamma_y K_{yy} + \eta_z \gamma_z K_{zz}\right) = D_{32w} \; ; \; D_{33w} = \frac{\lambda_w}{J_t}\left(\gamma_x^2 K_{xx} + \gamma_y^2 K_{yy} + \gamma_z^2 K_{zz}\right)$$

$$J_t = \left(x_\xi(y_\eta z_\gamma - y_\gamma z_\eta) - x_\eta(y_\xi z_\gamma - y_\gamma z_\xi) + x_\gamma(y_\xi z_\eta - y_\eta z_\xi)\right)^{-1}$$

where ξ_x, ξ_y, .., η_x, η_y, ..,γ_x, γ_y, … are the direct metrics of the transformation, which are evaluated numerically as a function of the inverse metrics (x_ξ, x_η, ..y_ξ, y_η, ..z_ξ, z_η,..). Expressions for direct metric as a function of the inverse metric can be found in Maliska (2004).

5. APPROXIMATE EQUATIONS

Equations (11) through (13) are integrated in the computational plane. Performing the integration of Eq. (11) in time and in the control volume of Fig. 1 and adopting a fully implicit method to evaluate the physical properties in each interface of the control volume, the following equation for the water component is obtained:
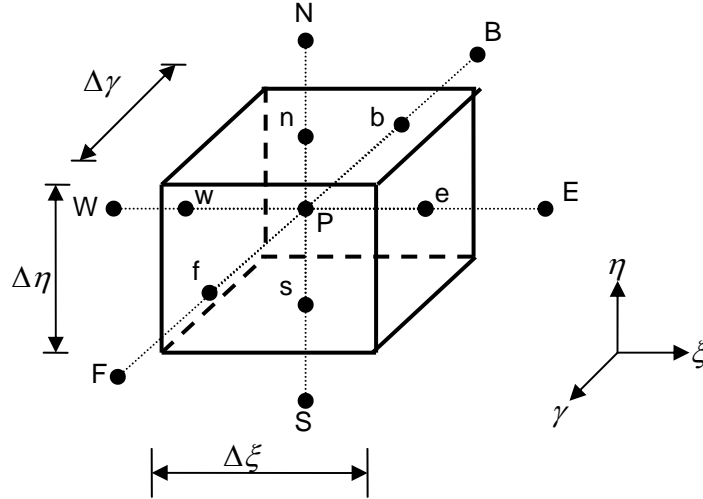

Figure 1 – Control volume in the computational plane

$$
\left[\left(\phi\rho_m Z_w\right)_P - \left(\phi\rho_m Z_w\right)_P^o\right]\left(\frac{\Delta V}{\Delta t\, J_t}\right)_P = \left(D_{11w}\frac{\partial\Phi_w}{\partial\xi} + D_{12w}\frac{\partial\Phi_w}{\partial\eta} + D_{13w}\frac{\partial\Phi_w}{\partial\gamma}\right)\Bigg|_e \Delta\eta\Delta\gamma - \left(D_{11w}\frac{\partial\Phi_w}{\partial\xi} + D_{12w}\frac{\partial\Phi_w}{\partial\eta} + D_{13w}\frac{\partial\Phi_w}{\partial\gamma}\right)\Bigg|_w ,
$$

$$
\left(D_{21w}\frac{\partial\Phi_w}{\partial\xi} + D_{22w}\frac{\partial\Phi_w}{\partial\eta} + D_{23w}\frac{\partial\Phi_w}{\partial\gamma}\right)\Bigg|_n \Delta\xi\Delta\gamma - \left(D_{21w}\frac{\partial\Phi_w}{\partial\xi} + D_{22w}\frac{\partial\Phi_w}{\partial\eta} + D_{23w}\frac{\partial\Phi_w}{\partial\gamma}\right)\Bigg|_s \Delta\xi\Delta\gamma +
$$

$$
\left(D_{31w}\frac{\partial\Phi_w}{\partial\xi} + D_{32w}\frac{\partial\Phi_w}{\partial\eta} + D_{33w}\frac{\partial\Phi_w}{\partial\gamma}\right)\Bigg|_f \Delta\xi\Delta\eta - \left(D_{31w}\frac{\partial\Phi_w}{\partial\xi} + D_{32w}\frac{\partial\Phi_w}{\partial\eta} + D_{33w}\frac{\partial\Phi_w}{\partial\gamma}\right)\Bigg|_b \Delta\xi\Delta\eta - \dot{m}_{wP}
$$

$$(15)$$

In Equation (15), $\dot{m}_{wP}$ is the mass flow rate of the water phase which is positive for the producing wells and negative for injecting wells. This term is given by

$$
\dot{m}_{wP} = \frac{\overline{m}_w\,\Delta V}{J_{tP}}
$$

$$(16)$$

The water mobility that is included in the D tensor is evaluated in each interface of the control volume using an upwind scheme. Considering, for instance, the interface lest of the control volume P (see Fig. 1) this mobility is evaluated by

$$
\lambda_{w,e} = \begin{cases} \lambda_{w,P} & se\ \left(G_{11}\frac{\partial\Phi_w}{\partial\xi} + G_{12}\frac{\partial\Phi_w}{\partial\eta} + G_{13}\frac{\partial\Phi_w}{\partial\gamma}\right)_e > 0 \\[2mm] \lambda_{w,E} & se\ \left(G_{11}\frac{\partial\Phi_w}{\partial\xi} + G_{12}\frac{\partial\Phi_w}{\partial\eta} + G_{13}\frac{\partial\Phi_w}{\partial\gamma}\right)_e < 0 \end{cases}
$$

$$(17)$$

The same procedure must me applied for the other interfaces of each control volume. The same procure performed to Eq. (11) must be realized to Eqs. (12) and (13). Next, the approximate equations need to be linearized. In this work, the Newton method was employed to linearize Eq. (15) and similar ones for the oil and pressure. All the 19 diagonals were kept at the linear system. As we have 3 unknowns per control volume, each entry in the matrix denotes a 3x3 sub-matrix. The linear systems were solved by the Bi-CGSTAB (van der Vorst, 1992) preconditioned with a right incomplete LU factorization of level 1, Marcondes et al (1985).

5. TEST PROBLEMS

In order to show the application of the methodology employed in the present work three case studies were carried out. The first one is the simulation of a saturated quarter of five spot. In this case, we injected water in order to increase the reservoir pressure and thus disappear the gas phase. For this case, only Cartesian meshes were employed. Table 1 presents the fluid and physical properties. The relative permeability curves for all study cases shown in this work are given in Tabs. 2 and 3. Also, the capillary pressure was set to zero in all simulated cases. The injection well is perforated along all layers while the producing well only in the first layer. From Table 1, it is possible to observe that oil and water phases are presented in the layer one and gas and water are presented in layer three.

Table 1 – Input data for case 1.

Reservoir data	Initial condition	Physical properties	Well conditions
$K = 9.9$ x 10^{-13} m^3 $A = 2.1404$ x 10^6 m^2 $\phi = 0.2$ $c_r = 0.0$ $r_w = 0.122$ m	$P = 20$ x 10^6 Pa $S_{wi} = 0.12$ $S_{oi} = 0.88$ (layer 1) 0.88 (layer 2) 0.00 (layer 3)	$B_w = 1$ at 0 Pa $c_w = 1.00$ x 10^{-10} Pa^{-1} $c_o = 1.985$ x 10^{-9} Pa^{-1}	$q_{wi} = 17280$ m³/d $P_{wf} = 20$x10^6 Pa

Table 2 – Oil-gas relative permeability as a function of liquid saturation ($S_w + S_o$).

S_{lt}	k_{rg}	k_{rog}
0.00000	0.984	0.0000
0.03409	0.980	0.0000
0.20454	0.940	0.0000
0.31818	0.870	0.0004
0.43182	0.720	0.0010
0.48864	0.600	0.0100
0.54545	0.410	0.0210
0.65909	0.190	0.0900
0.71591	0.125	0.2000
0.77273	0.075	0.3500
0.86364	0.025	0.7000
0.94318	0.005	0.9800
0.97727	0.000	0.9970
0.99886	0.000	1.0000

Table 3 – oil-water relative permeability as a function of water saturation (S_w).

S_w	K_{rw}	K_{ro}
0.12	0.00	1.00
0.82	1.00	0.00

The second case study refers to an undersaturated reservoir in a quarter-of-five-spot. For this case study, Cartesian and boundary fitted coordinates were employed. The reason for the non-orthogonal mesh be used here is to investigate the boundary fitted implementation. It is worthwhile to mention that the reservoir production does not depend on the way the reservoir was discretized and the approximate equations were solved. On the other hand, the numerical results are strongly affected by the employed meshes and the way the equations are solved. For this case, only the primary recovery is investigated through the use of two producing wells perforated in all three layers of the reservoir. The input data for this case study case is shown in Tab. 4. Figure 2 shows the boundary fitted mesh employed to this case study.
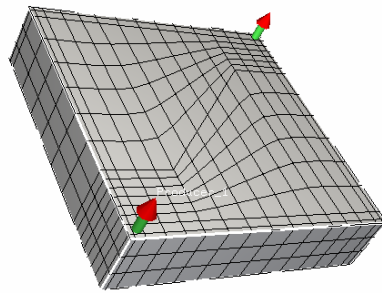
Figure 2 – Case study 2 – 16x16x3 boundary fitted mesh.

The last case study refers to a reservoir with a more complex geometry. Figure 3 presents the reservoir. As the IMEX code does not include the cross derivatives in the mass flow rate evaluation, the results for this case study are not compared with the IMEX simulator. Table 5 presents the input data used. This case study also refers to undersaturated reservoir and only the primary recovery is investigated.

Table 4 – Input data for case 2.

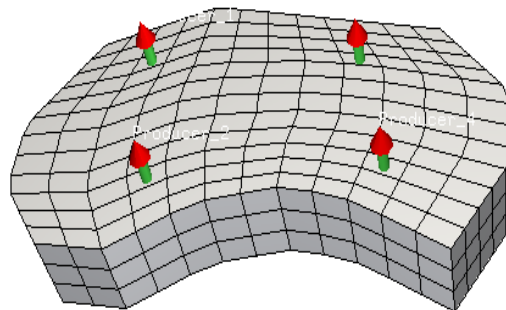| Reservoir data	Initial condition	Physical properties	Well conditions
$k = 9.9 \times 10^{-13}$ m^3 $h = 15$ m $A = 2.1404 \times 10^6$ m^2 $\phi = 0.2$ $c_r = 0.0$ $r_w = 0.122$ m	$P = 33065.3 \times 10^3$ Pa $S_{wi} = 0.12$ $S_{oi} = 0.88$	$B_w = 1$ at 0 Pa $c_w = 1.00 \times 10^{-10}$ Pa^{-1} $c_o = 1.985 \times 10^{-9}$ Pa^{-1}	$P_{wf} = 20 \times 10^6$ Pa

Figure 3 – Case study 3 – 12x12x3 boundary fitted mesh.

Table 5 – Input data for case 3.

Reservoir data	Initial condition	Physical properties	Well conditions
$k = 9.9 \times 10^{-13}$ m^3 $h = 30$ m $A = 40.59 \times 10^6$ m^2 $\phi = 0.2$ $c_r = 0.0$ $r_w = 0.122$ m	$P = 33065.3 \times 10^3$ Pa $S_{wi} = 0.12$ $S_{oi} = 0.88$	$B_w = 1$ at 0 Pa $c_w = 1.00 \times 10^{-10}$ Pa^{-1} $c_o = 1.985 \times 10^{-9}$ Pa^{-1}	$P_{wf} = 20 \times 10^6$ Pa

6. RESULTS

All the results shown in this section were obtained with the following criteria for the convergence of the solution in each time-step, in pressure and in global mass fraction of oil and water, respectively: 68,947.57 Pa (10 psi) and 5×10^{-4}. Figure 4 presents the cumulative production of oil, gas, and water for case study 1. From Figure 1, it is possible to observe that a good agreement between the present formulation and the commercial simulator IMEX were obtained.
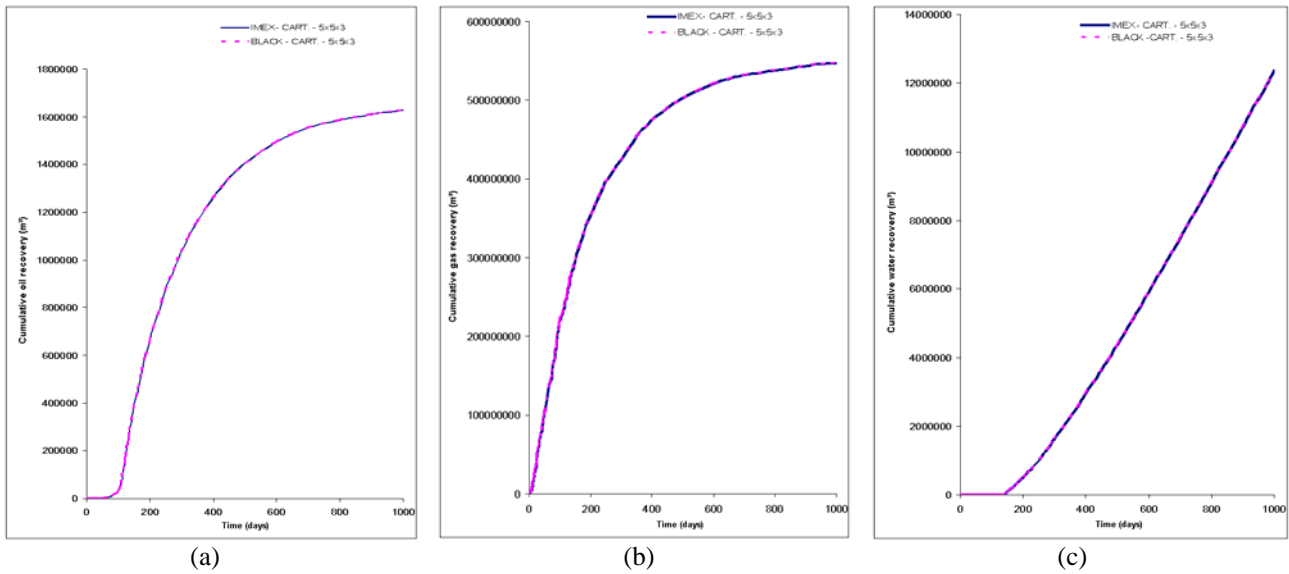
(a) (b) (c)

Figure 4 – Cumulative production rates – case study 1. a) oil b) gas c) water

The cumulative production rate for case study 2 are shown in Fig. 5, for Cartesian, boundary-fitted coordinates, and IMEX using Cartesian mesh. As can be seen from Fig. 5, a good agreement between the results obtained with the present formulation for all the tested meshes were obtained. Also, the results are again very close to the ones obtained with the commercial simulator IMEX.
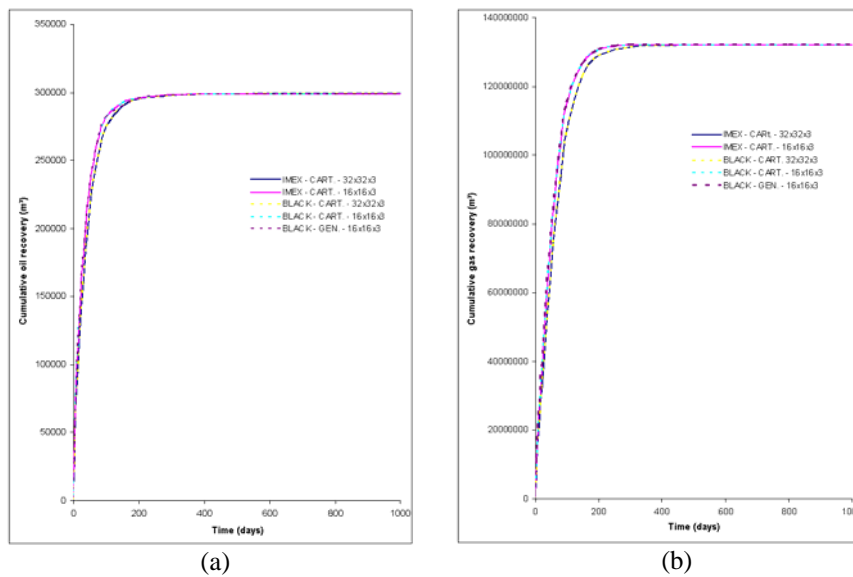

(a) (b)

Figure 5 – Cumulative production rates – case study 2. a) oil b) gas

Figure 6 shows the gas saturation field in 43, and 98 days. From this figure, it is possible to observe that the gas phase appears just around the producing wells in the first days of producing, and later on, due to the lowest density of the gas phase the whole gas phase are concentrated in the top of the reservoir (third layer).

Figure 7 presents the total volumetric rates of oil and gas for the third case study. For this case, two boundary fitted coordinates meshes are employed. For the reason mentioned previously, we have not compared the results of the present work with the commercial simulator IMEX. As can be seen in Figure 7, good agreements were obtained for both mesh configurations.
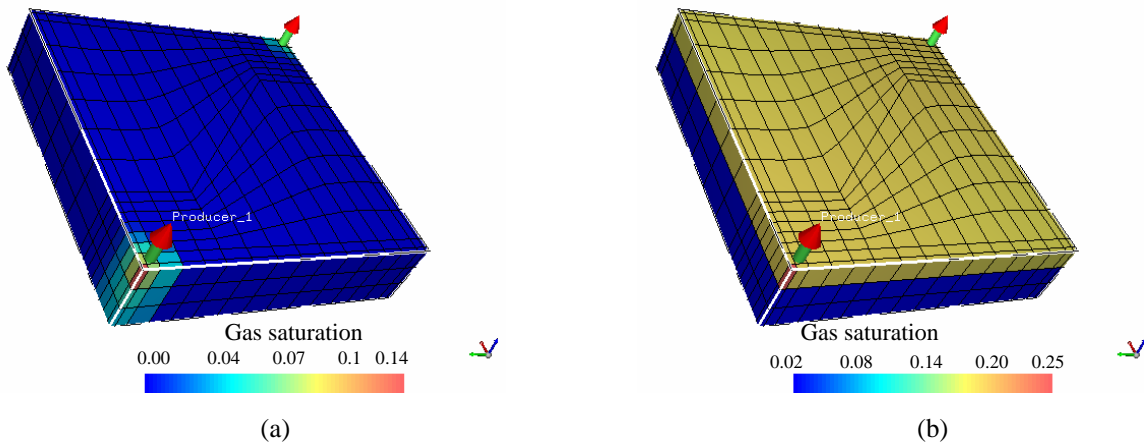
(a)

(b)

Figure 6 – Gas saturation field – case study 2. a) 43 days b) 98 days
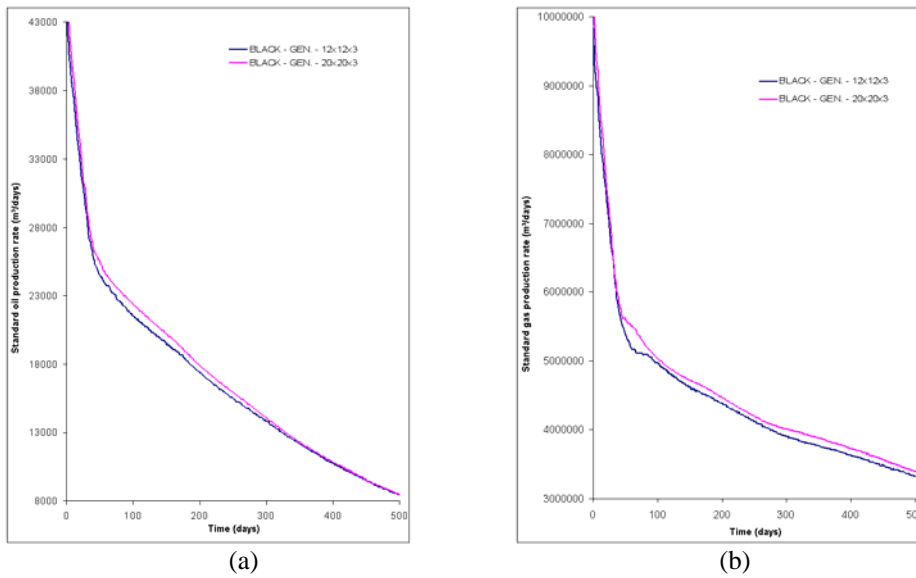

(a)

(b)

Figure 7 – Cumulative production rates – case study 3. a) oil b) gas

Figure 8 presents the gas saturation field in 41 and 64 days, and Fig. 9 presents the gas saturation field in 97 and 157 days obtained for case study 3.
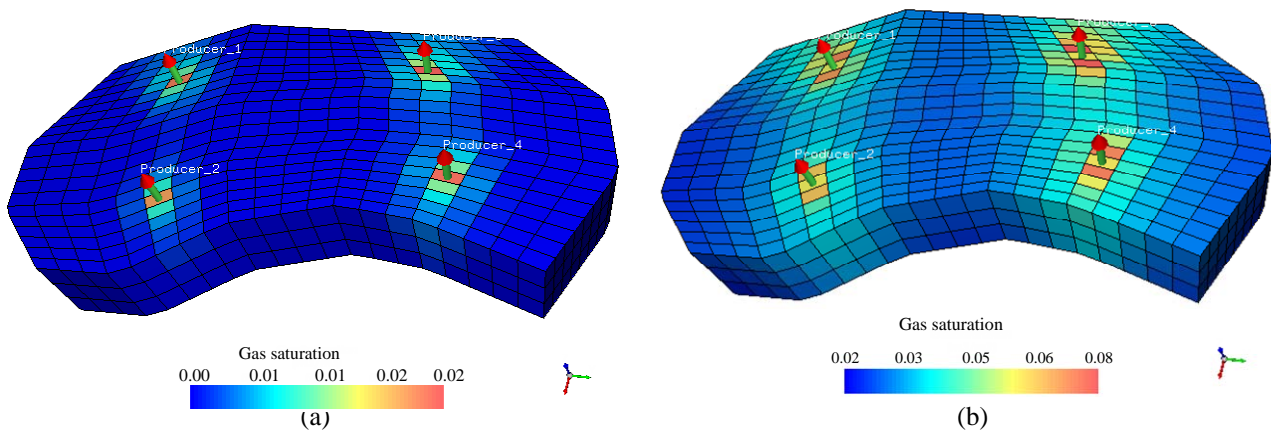

(a)

(b)

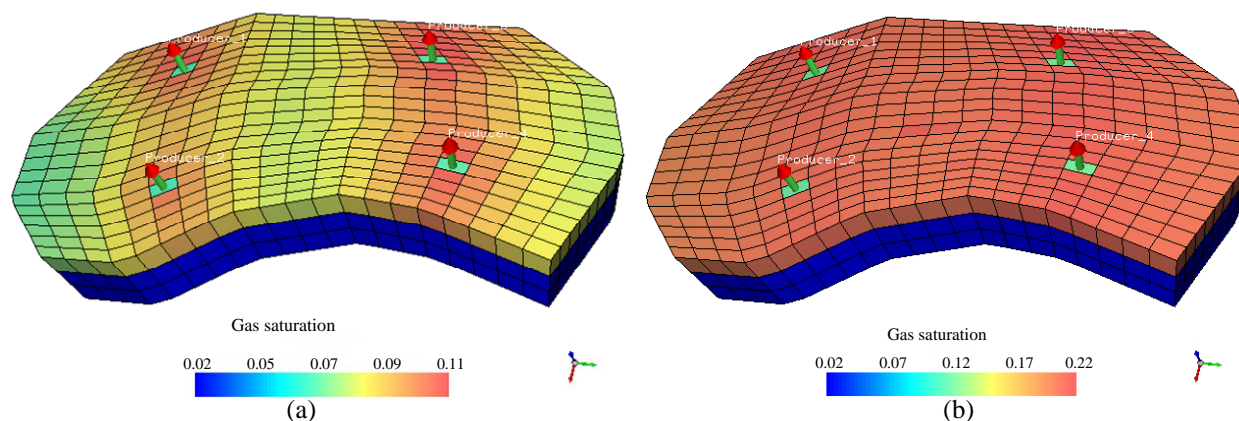Figure 8 – Gas saturation field – case study 3. a) 41 days b) 64 days

Figure 9 – Gas saturation field - case study 3. a) 97 days b) 157 days

Again, from Figures 8 and 9 it is possible to observe the same behavior already seen for the gas saturation for case study 2. We mean, at the begin, the gas phase come out of the solution of oil phase and then quickly spreads out all over the last layer of the reservoir, due to the lowest density of the gas phase compared to the oil and water phases.

7. CONCLUSIONS

The present work has implemented and tested the black-oil model based on global mass fraction and pressure in conjunction with boundary fitted coordinates. The equations were solved by the finite volume method using a fully implicit formulation. The implemented formulation was able to treat the gas phase appearance and disappearance without any additional numerical tricks as occurs with the traditional black-oil formulation based on saturations and pressure for several saturated and undersaturated reservoirs.

8. ACKNOWLEDGEMENTS

The authors would like to to thank CNPq (The National Council for Scientific and Technological Development of Brazil) for their financial support.

9. REFERENCES

Cunha, A. R. C., 1996 "Methodology for 3D Petroleum Reservoir Simulation Using the Black-oil Model and Mass Fraction Formulation", M.Sc. Thesis (in Portuguese), Federal University of Santa Catarina, Florianópolis, Brazil.
Maliska, C. R., 2004, "Computational Heat Transfer and Fluid Flow", 2nd Edition (in Portuguese), Livros Técnicos e Científicos Editora S.A., Rio de Janeiro, Brazil.
Maliska, C.R., da Silva, A.F.C., Czesnat, A.O., Lucianetti, R.M., and Maliska Jr., C.R., 1997, "Three-Dimensional Multiphase Flow Simulation in Petroleum Reservoirs using the Mass Fractions as Dependent Variables", SPE 39067-MS, Latin American and Caribbean Petroleum Engineering Conference, Rio de Janeiro, Brazil.
Marcondes, F., Zambaldi, M. C., Maliska, C. R., 1985, Comparison of Non-Stationary Methods Using Unstuctured Voronoi Mesh in Petroleum Simulation" (in Portuguese), XII COBEM, Belo Horizonte, Brazil.
Prais, F. and Campagnolo, E. A., 1991, "Modeling of Multiphase Flow in Reservoir Simulation" (in Portuguese), XI COBEM, São Paulo, Brazil.
Thomson, J. F., Warsi Z. U. A., and Mastin, C. W., 1985 "Numerical Grid Generation –Foundation and Applications", Elsevier Sciennce Publishing Co., EUA.
van der VORST, H. A., 1992, "BI-CGSTAB: A fast and smoothly converging variant of Bi-CG for the simulation of nonsymmetric linear systems, SIAM J. Sci. Stat. Compt., 13, pp. 631-644.

10. RESPONSIBILITY NOTICE

The authors are the only responsible for the printed material included in this paper.